Utilization of a mixture of CTs and current sensors in line differential protection applications

Author(s): Raipala, Ontrei; Hovila, Petri; Leminen, Janne; Farughian, Amir; Memon, Aushiq; Kauhaniemi, Kimmo

Title: Utilization of a mixture of CTs and current sensors in line differential protection applications

Year: 2019

Version: Publisher's PDF

Please cite the original version:

Raipala, O., Hovila, P., Leminen, J., Farughian, A., Memon, A., & Kauhaniemi, K., (2019). Utilization of a mixture of CTs and current sensors in line differential protection applications. In: *Proceedings of 25th International Conference on Electricity Distribution: CIRED 2019 : Madrid, 3-6 June 2019*, paper 292. https://www.cired-repository.org/handle/20.500.12455/808

UTILIZATION OF A MIXTURE OF CTS AND CURRENT SENSORS IN LINE DIFFERENTIAL PROTECTION APPLICATIONS

Ontrei RAIPALA
ABB Oy – Finland
ontrei.raipala@fi.abb.com

Petri HOVILA
ABB Oy – Finland
petri.hovila@fi.abb.com

Janne LEMINEN
ABB Oy – Finland
janne.leminen@fi.abb.com

Amir FARUGHIAN
University of Vaasa – Finland
amir.farughian@uwasa.fi

Aushiq MEMON
University of Vaasa – Finland
amemon@uwasa.fi

Kimmo KAUHANIEMI
University of Vaasa – Finland
kimmo.kauhaniemi@uwasa.fi

ABSTRACT

The popularity of Rogowski sensors is increasing due to their advantages over conventional CTs. Consequently, network utilities may sometimes end up facing a question whether it would be possible to use line differential protection on a line where the current measurements at the local end are based on CTs, whereas, the remote end measurements are based on current sensors. The main challenge in the use of such a combination in line differential protection applications is that while CTs may saturate, Rogowski sensors do not. Such issues were studied in a hardware-in-the-loop simulation setup. Based on the studies conducted, it appears that the use of mixture of CTs and current sensors for line differential protection applications is a feasible option provided that the CTs are properly dimensioned and that the protection settings are carefully chosen.

INTRODUCTION

The current differential protection is the most preferred choice for protection of individual power system components (lines, generators, transformers etc.) as the main protection because of its 100% selectivity and fast response to the internal faults (the faults within the protected zone). Since the location of current transformers (CTs) defines the boundary of the protected zone, time grading with other protection systems is not required which inherently helps tripping without an additional delay. Extremely fast tripping time of less than one cycle is possible for the internal faults with proper dimensioning and matching of CTs. However, current differential protection also has few shortcomings. That is, it does not provide backup protection for the next line (in case of line differential protection), a communication link between line terminals is necessary and it may suffer from false tripping in the event of CT saturation. The principle of operation of modern current differential protection is simple and straightforward; the currents at both ends of protected zone are measured and compared inside the numerical relays at each end. The measured values of current at one end are digitally coded and transmitted to the other end via a dedicated fiber optic cable. The vector sum of currents at both ends should be ideally zero according to Kirchhoff's current law for the normal operation without any fault. However, in practice there is always some magnitude of differential current present due to CT errors, charging currents of cables, synchronisation errors etc. Events like high magnitude of fault current causing CT saturation, the modification of the transformation ratio due to transformer tap changers and external faults (faults outside the protected zone) may produce additional false differential current and may result in mal-operation of differential protection. Consequently, a biased or stabilized differential protection is required for the most practical applications [1]. Modern line differential protection functions typically include a stabilized low stage and an instantaneous high stage [1], [2]. The stabilized low stage ensures high sensitivity while yet remaining stable, for instance, during CT saturation. The instantaneous high stage is less sensitive but, on the other hand, enables rapid clearance of faults during high fault currents. Direct intertrip function, which ensures that both ends are always simultaneously tripped, is also included in some IEDs [2].

Electric distribution networks are highly capital intensive. The lifetime of primary network components is fairly long spanning to several tens of years. Distribution network operators therefore prioritize their investments according their unique development needs and make improvements in the primary network infrastructure only in chosen parts annually. Thus, it is not uncommon that while one of the substations is renewed, the neighboring substations are not renewed at the same time. Situations like this can lead to a question whether it would be possible to continue applying line differential protection for the protection of a distribution line between two neighboring substations, of which one utilizes current sensors while the measurements at the other end of the line are based on CTs. This paper studies whether this kind of mixture of current sensors and CTs can be used for line differential protection without jeopardizing the dependability and security of protection.

CTS AND CURRENT SENSORS

Previously, the Rogowski coil sensors were only used in expensive laboratory equipment. But due to the advancement of the modern numerical relays, also called the intelligent electronic devices (IEDs), the applications of Rogowski coil current sensors are also increasing in standard switchgear. A Rogowski coil current sensor is an air-core coil, a toroidal coil without an iron core placed around the primary conductor in the same way as the secondary winding in a conventional CT. But the output signal from the Rogowski coil current sensor is different from a conventional CT. The output signal from the current sensor is a "voltage signal" which is proportional to the derivative of the primary current, whereas the output from a conventional CT with its iron core and nearly short-circuited secondary winding is a "current". This secondary current is proportional to the primary current. Due to the absence of iron core in a Rogowski coil, no saturation occurs in current sensor and the output is linear over the whole current range up to the highest currents. Due to no saturation, current sensors are more accurate than the conventional CTs. However, the IEDs should be capable of operating accurately at low input signal levels of current sensors. The other advantages of current sensors include: no calculation of accuracy versus burden, compact design hence current and voltage sensors can be combined in one sensor, no safety hazard to personnel and equipment due to low voltage output (10 V) etc. [3][4].

The main challenge in using a combination of CTs and sensors in line differential protection applications is lies in the fact that CTs may saturate whereas currents sensors do not. Thus, if the utilized CTs at local end saturate while current sensors at the remote end do not saturate, an erroneous differential current caused by the differences in measurements is introduced even if the fault would be external. Should the CTs saturate significantly, a potential risk of unwanted tripping during external faults is evident. There appears to be very limited if any studies concerning this issue in the literature. This paper aims to fill this gap by providing experimental studies analyzing the feasibility of utilizing a combination of CTs and current sensors for line differential protection applications.

SIMULATION MODELS

The simulations are carried out in the Simulink environment with the help of the real time simulator Opal-RT and its hardware in the loop (HIL) feature. The simple network modelled for the tests is shown in Figure 1. It consists of a short cable feeder J02 (850m of AHXAMK-W 3x240) and another feeder J01. A 3.6 MW full-converter wind turbine is connected to the tail part of J02. The network model is capable of providing 5.2 kA fault current in case of a three-phase short circuit at the beginning of J02.

Two actual differential protection relays are set to protect the short feeder. The local relay located at the beginning of J01 receives its measurements from CTs, whereas, the remote IED gets its measurements via real current sensors. The CT model used in this study is KOFD 12A41 5P10 300 / 1 A CT with a 20 VA nominal burden. It is modeled accurately using magnetization curve shown in Figure 2.

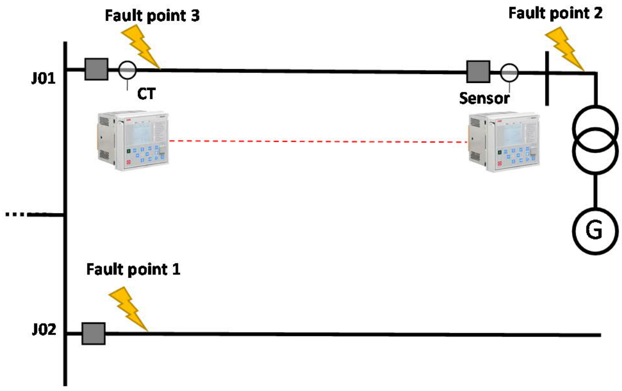

Figure 1. The modelled feeders of the studied network.

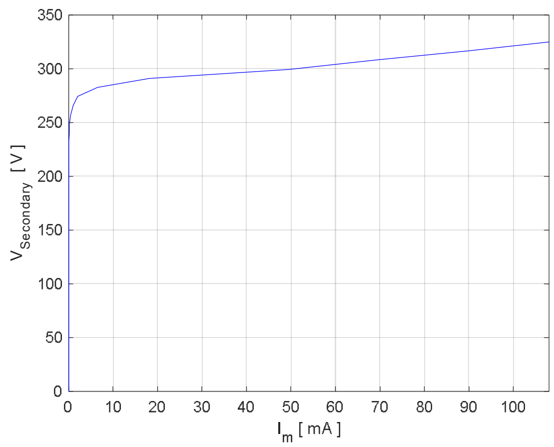

Figure 2. CT magnetization curve

TEST SETUP

The studies of this paper are based on a hardware-in-the-loop laboratory setup consisting of a real-time simulator, two amplifiers, real Rogowski current sensors and real line differential protection (ABB RED615) IEDs which interact with each other in the manner shown in Figure 3.

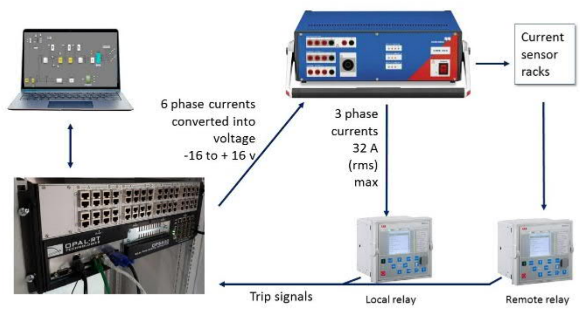

Figure 3. Interaction between Opal-RT, sensor racks, amplifiers and relays

First, the model built in Simulink is uploaded to Opal-RT. The measurements made by the CT models in the simulation model are output via the analog output port of Opal-RT. As these outputs are in the form of voltage, an amplifier converts these signals into currents with proper scaling and feeds the local relay. Similarly, the measurements seen at the remote end are fed first to the sensors installed in a special rack using an amplifier and then the measurements from sensors are brought to the remote relay. The trip signals of both relays are taken to the inputs of Opal-RT and recorded.

To create currents that are as high currents as sensors sense on an actual feeder, two amplifiers are needed. In addition, the sensors are fitted in sensor racks so that there are 80 rounds of wire going through the sensors. Therefore, the sensors sense 80 times the current that the amplifiers provide. The actual hardware-in-the-loop simulation setup in the laboratory of University of Vaasa is shown in Figure 4.

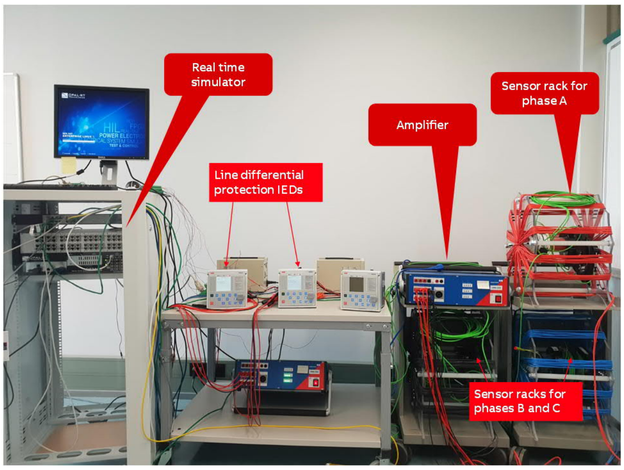

Figure 4. Utilized hardware-in-the-loop simulation setup

The utilized differential current IEDs calculate the differential current I_{diff} and stabilizing current I_{bias} at both line ends as formulated in equations 1 and 2.

$$I_{diff} = |\bar{I}_{LOCAL} + \bar{I}_{REMOTE}| \qquad (1)$$

$$I_{bias} = |\bar{I}_{LOCAL} - \bar{I}_{REMOTE}|/2 \qquad (2)$$

,where I_{LOCAL} and I_{REMOTE} are the fundamental frequency components of local and remote end currents phasors.

SIMULATION CASES AND RESULTS

When a CT-sensor combination is used, there is a concern that the relays might issue a false trip signal when there is a fault outside of the protected zone due to CT saturation. To investigate the possibility of using CT-sensor combination, the following cases are studied:

1. CT-sensor in case of an internal fault

   In this case, faults NO. 3 marked on Figure 1 occurs. As this fault is in the protected zone, the relays are expected to trip.

2. CT-sensor in case of an external fault

   In this case, faults NO. 1 and 2 marked on Figure 1 occur. As these faults are located outside of the protected zone, the relays are expected not to trip.

3. External faults with incorrectly dimensioned CTs

   The purpose of this case is to test the protection security of differential protection during external faults with an incorrectly chosen CT on the local end. The CT model used in this case is the same CT but with the difference that the burden is increased in order to degrade the CT performance (i.e. the CT dimensioning is not in line with ABB CT specification for line differential protection applications).

For all the tests performed in this paper, the fault resistance is set to 0.01 Ω line-to-line. The tests were carried out with different fault types (two—phase and three—phase) and varying inception angles (0◦ & 90◦ leading). However, in this paper, only few interesting cases are presented with more details due to the lack of space.

Case 1. Internal L1-L2-L3 fault

The first presented case illustrates the functioning of differential protection during an internal three phase fault when the local end measurements are obtained via CTs while the remote end measurements are obtained via current sensors. The uppermost graph in Figure 5 illustrates the behaviour of phase L1 local- and remote end currents during an internal three phase short circuit. As it can be seen from the graph, a certain degree of CT saturation occurs. However, this is not of significant importance due to the large difference in the local and remote end currents during this internal fault. The lowermost graph in Figure 5 presents the resulting phase L1 differential current as seen by the IEDs.

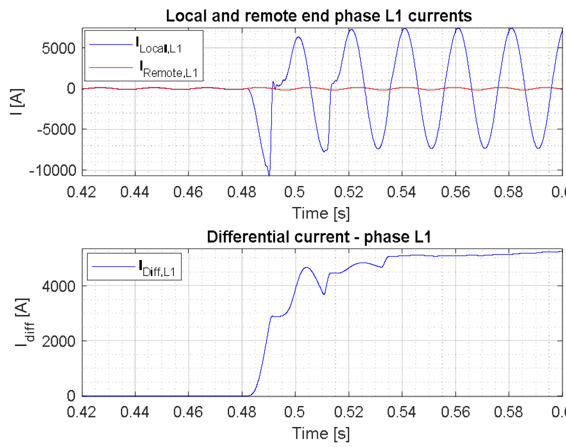

Figure 5. Local and remote end phase L1 currents during an internal three phase fault at the beginning of the feeder and the resulting differential current as seen by the IEDs

Figure 6 presents the resulting secondary fault current trajectories in a stabilizing current (I_{bias}) versus differential current (I_{diff}) coordinate system as seen by the IEDs from the same case. The axes in the graph are given in relation to the rated current of the current sensors, which was 250A. The dashed lines in the figure represent the utilized thresholds for differential protection. As it can be seen from the graph, the fault current trajectories exceed both the low- and the high stage thresholds. Consequently, differential protection tripped and the OPAL-RT simulator recoreded operation times equal to 30ms (local end) and 32ms (remote end).

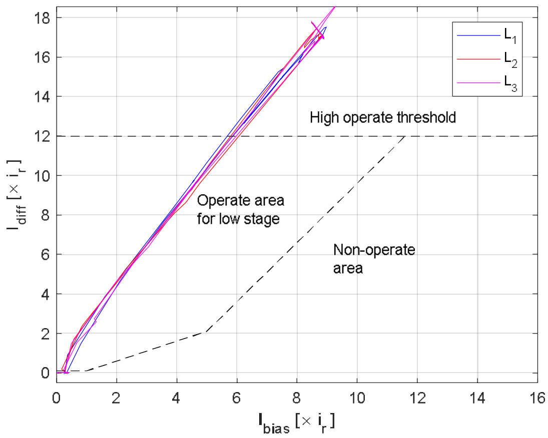

Figure 6. The fault current trajectories of Figure 5 in an I_{bias} versus I_{diff} coordinate graph as seen by the IEDs

Case 2. External L1-L2 fault

This case illustrates how the differences in current measurement principles may cause differential protection to see a large differential current during external faults when the CTs on the local end saturate. The studied fault type in this case was a two phase short circuit (L1-L2) and the fault was located at the tail of the feeder (fault point 2 in Figure 3). As the uppermost graph in Figure 7 illustrates, a significant degree of saturation occurs in phase L2 current measurement at the local end CT during the beginning of the fault. The current sensors at the remote end naturally do not saturate. Consequently, as the lowermost graph in Figure 7 illustrates, the resulting differential current seen by the relays is as high as 800 A although the fault is external. Despite the high differential current shown in Figure 7, no tripping occurs due to the high stabilizing current (I_{bias}). This is illustrated more in detail in Figure 8, which presents I_{bias} versus I_{diff} fault current trajectories formulated from the fault recordings of the relays. Note that the currents in Figure 8 are in reference to the sensors rated current 250A. The blue coloured arrows illustrate the temporal behaviour of the fault current trajectories. As the figure illustrates, the fault current trajectories do not exceed the utilized thresholds and no tripping thus occurs.

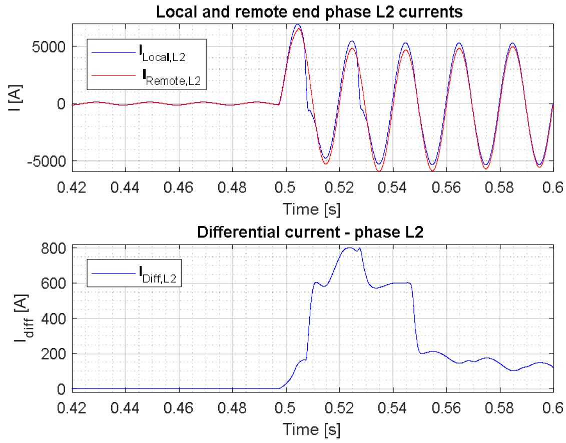

Figure 7. Local and remote end phase L2 currents during an external L1-L2 fault at fault point 2 and the resulting differential current as seen by the IEDs

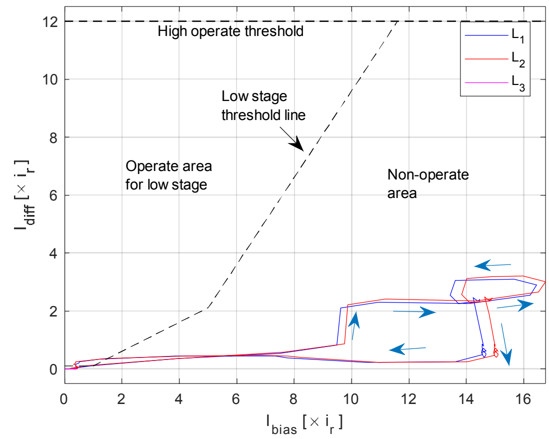

Figure 8. The fault current trajectories of Figure 7 in an I_{bias} versus I_{diff} coordinate graph as seen by the IEDs

Case 3. External fault with improper CT

The following case illustrates how improperly sized CTs may lead to protection security problems during external faults. For the studied case in question, the actual accuracy limit factor K'_{alf} of the CTs should be equal or larger than 30 according to the CT selection guidelines given in [5]. However, in order to illustrate the potential problems, incorrectly sized CTs were used in the following case. In this case the CTs K'_{alf} was 8.47, which is way below the instructed minimum K'_{alf} value 30. Due to the incorrect CT sizing, a significant degree of CT saturation occurs in the local end during the fault. As the Rogowski sensors at the remote end do not saturate, large differential currents are formed as a consequence of the differences in current measurements as shown in Figure 9. The resulting fault current trajectory of phase L1 is shown in Figure 10. Now the fault current trajectory of phase L1 exceeds the utilized differential protection thresholds and consequently an unwanted tripping occurs in circa 39ms after the beginning of the fault. It is noteworthy that no tripping occurred when the current sensors at the remote end were replaced by the same incorrectly sized CTs and the test was repeated. This highlights the importance of using properly sized CTs especially in line differential protection applications based on a mixture of CTs and current sensors.

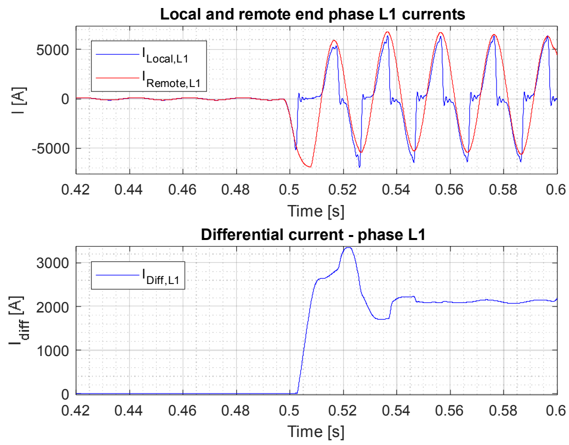

Figure 9. Local and remote end phase L1 currents during an external three phase fault at fault point 2 and the resulting differential current as seen by the IEDs

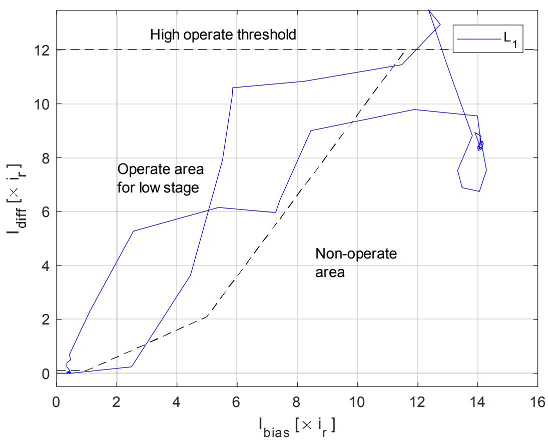

Figure 10. The fault current trajectories of Figure 9 in an I_{bias} versus I_{diff} coordinate graph as seen by the IEDs

DISCUSSION

CT dimensioning guidelines given by relay manufactures are typically designed for applications where CTs are used at both ends. Thus, there may not always be sufficient safety margin present in the CT dimensioning principles for the utilization of differential protection based on a mixture of CTs and current sensors. Consequently, typical CT dimensioning guidelines do not necessarily consider sufficient margin for applications utilizing a mixture of CTs and current sensors. This is especially important to bear in mind from protection security point of view because large differential currents could be seen by the IEDs during external faults when the CTs on the one end saturate while the currents sensors at the other end do not. However, the CT selection guideline utilized in this study seemed to include sufficient margin for ensuring secure operation in the conducted studies.

The current magnitudes in the studied test setup and model had to be limited to a modest level due to the limitations with the utilized current amplifiers. That is, the resistance of the sensor rack, in which the conductor was wound 80 times through the Rogowski sensor, caused such a high burden to the amplifiers that no higher currents could be applied in the test setup. If similar type of studies were to be done with considerably higher currents, it could be more sensible to use an accurate model of sensors instead. This is because a hardware-in-the-loop simulation setup may be impractical due to the very high requirements of amplifiers output capacity in terms of power and current.

CONCLUSIONS

This paper analysed the feasibility of using a mixture of CTs and current sensors in line differential protection applications. The studies were based on tests conducted in a laboratory test setup consisting of a real-time simulator, commercial Rogowski current sensors and line differential protection IEDs. With the help of this unique test setup, it was possible to study the functioning of line differential protection realistically in cases where the measurements are based on a mixture of CTs and current sensors. Based on the conducted experimental studies, it appears that the use of a mixture of CTs and current sensors could be a feasible option in line differential protection applications without endangering protection dependability or security. However, it is crucial to ensure that the CTs are correctly dimensioned and protection settings are chosen carefully.

REFERENCES

[1] Gerhard Ziegler, Numerical Differential Protection Principles and Applications, Sec Ed, Publicis Publishing, Erlangen, 2012.

[2] ABB Product Guide, RED 615 Line Differential Protection and Control, 1MRS756500 M, 2018. https://library.e.abb.com/public/2d859983e9af4783927a8174b2c18664/RED615_pg_756500_ENm.pdf?x-sign=iQg8zAifpoCPuFyGMKrU+DSwQHAqcAm8KWQBoSDi7IxH8JJKCow3CHc7lZlYhN/P

[3] Sensor Technology Applications for medium voltage, https://library.e.abb.com/public/1e128df13ad6ea51c1257b1300572968/sensor1GB%200211.pdf

[4] Revolution in measuring techniques enables superior protection performance https://library.e.abb.com/public/435d28e6077fec47c2256c3e002c24ed/ElectricityInternational.pdf

[5] ABB Oy. Technical Note 1MRS756965EN rev. B, 2009, *CT Selection in RED615 Applications*.